Materials Physics and Mechanics. 2022;50(1): 166-183
Research article
http://dx.doi.org/10.18149/MPM.5012022_13

Submitted: April 30, 2022
Approved: July 12, 2022
Accepted: August 12, 2022

The effect of phase lags and fractional parameters on waves across an elastic and thermoelastic medium

Puneet Bansal[1], Vandana Gupta[2]✉

[1]University Institute of Engineering and Technology, Kurukshetra University Kurukshetra, Haryana, India

[2]Department of Mathematics, IGN College, Ladwa, Haryana, India

✉ vandana223394@gmail.com

Abstract. In this paper, three-phase lag heat transfer model Roychoudhari [1] is employed to study the problem of reflection and transmission of thermoelastic waves of an obliquely incident plane P or SV wave at the interface between an elastic solid and a fractional order thermoelastic solid subjected to continues boundary conditions. The amplitude reflection and amplitude transmission coefficients are derived by using the potential method. It was found that the energy ratios and amplitude ratios of waves depend upon the incident angle and the frequency of the incident wave. The problem is illustrated by computing numerical values of amplitude ratios and energy ratios for the copper material. Graphical results for two-phase lag are compared with the corresponding results for three-phase lag theory of thermoelasticity. The effect of fractional order on the energy ratios is also discussed graphically. The present derivation is used to study the energy conservation among the incident, reflected, and transmitted waves. It is verified that in this process there is no energy dissipation at the interface.

Keywords: amplitude; fractional, reflection, transmission, three-phase lag, elastic waves, energy ratio

***Acknowledgements**. No external funding was received for this study.*

Citation: Bansal P, Gupta V. The effect of phase lags and fractional parameters on waves across an elastic and thermoelastic medium. *Materials Physics and Mechanics*. 2022;50(1): 166-183. DOI: 10.18149/MPM.5012022_13.

1. Introduction

The field of fractional calculus studies fractional derivatives, fractional integrals, and their properties. Fractional calculus is the mathematical study that takes the traditional definitions of integral and derivative operators of calculus to the fractional integral and derivatives. Although there was not any geometrical and physical representation of fractional order integral and derivatives for more than 300 years. Igor Podlubny showed the geometric interpretation and physical representation as "Shadows on the walls" and "Shadows of the past" respectively.

Fractional calculus is used in many desirable models to review the physical processes considerably among with heat conduction, diffusion, viscoelasticity, solid mechanics, electrical networks, fluid flow and electromagnetic theory, etc. which involves integrals and derivatives of fractional order. In many cases the use of fractional order theory is very useful in situations where the heat conduction law depending upon classical theory fails.

Abel [2] was the first to use fractional calculus for the tautochrone problem. It can be stated that the theory of fractional derivatives and integrals was established after the 1950's. Caputo and Mainardi [3-4] and Caputo [5] experimentally verified the use of fractional derivatives for viscoelastic materials and proved the connection between fractional derivatives and linear viscoelasticity. Miller and Ross [6] established a collection of various developments and applications in the field of fractional calculus.

The path of transformation in the heat equation law of classical theory to the parabolic type heat conduction equation was opened by Lord and Shulman [7]. A further modification was made by Green and Naghdi [8-10] by the introduction of three distinct theories. Chandrasekharaiah [11] introduced the dual phase lag theory of thermoelasticity. This theory supported the theory proposed by Tzou [12-13] where the heat conduction equation becomes hyperbolic. In this model heat conduction equation involves two-phase lags to study the microstructural effects that occur during the heat transfer. The theory given by Roychoudhuri [1] was the modification of the previous generalized theories of thermoelasticity and it involves a Fourier law having three phase lags.

Achenbach [14] described the different aspects of elastodynamics and wave propagation phenomenon for thermoelastic solid medium. Borcherdt [15] studied the reflection and refraction of waves in elastic and anelastic solid mediums. Sherief and Saleh [16] using the Laplace Transform technique studied a half-space problem in a generalized thermoelastic diffusion medium. Kumar and Gupta [17-18] in their work used the methodology of fractional calculus and dual-phase-lags. Wang, Liu, Wang & Zhou [19] derived the basic equations for anisotropic temperature-dependent generalized thermoelastic medium with fractional order parameters.

Raslan [20] using the Laplace transform technique solved a one-dimensional problem having fractional derivative and computed the results for temperature change, displacement, and stress distribution. Abbas [21] studied the coupling of plasma, elastic and thermal waves using the eigenvalue approach. He also depicted the difference between the classical, Lord-Shulman and the dual phase lag theory. Lata [22] studied the thermomechanical interactions in a thick circular plate under the two temperature theory of thermoelasticity with fractional order derivative. Kumar, Vashisth, and Ghangas [23] investigated the effect of phase lag, two-temperature, and void on waves in the anisotropic thermoelastic medium.

Atwa and Ibrahim [24] studied the effect of two temperatures and diffusion and also depicted the effect of three-phase lag and Green Nagdhi type III theories of thermoelasticity. Nonlocal theory having fractional derivative heat transfer thermoelastic medium with voids was studied by Bachher and Sarkar [25].

Waves in a thermoelastic medium with dual-phase-lag and voids were studied by Mondal, Sarkar, and Sarkar [26]. Said [27] used fractional order parameters to study the plane wave propagation and computed the fundamental solution.

Abouelregal [28] used the theory of fractional calculus and derived a new model of three-phase-lag thermoelastic heat conduction of higher-order time-fractional derivatives that includes high-order time-fractional derivative approximations of three-phase-lags in the heat flux vector, the temperature gradient and in the thermal displacement gradient.

Abouelregal and Ahmad [29] constructed a fractional order thermoelastic model with phase lags. Saidi and Abouelregal [30] studied the thermoelastic model for an infinitely long cylinder with two phase-lags having higher-order time-derivatives.

Kulkarni and Mittal [31] applied the two-temperature theory to a homogeneous isotropic generalized dual phase lag fractional order thermoelastic medium. He obtained thermal displacement, stresses, conductive temperature, and thermomechanical temperature using the State space approach.

Abouelregal et al. [32] established a generalized thermoelastic model by considering two-fractional thermal conduction and multi-phase-lags. They also extracted several models of generalized thermoelasticity including fractional derivatives from the considered model.

Abouelregal et al. [33] presented a new fractional model of non-Fourier heat conduction that includes phase delays and two fractional orders using the Laplace transform approach. Sharma [34] studied the effect of phase-lags and voids on thermoelastic interactions in a nonlocal elastic hollow cylinder.

The present paper is concerned with the reflection and transmission phenomena of the P and SV waves striking at the plane interface between an elastic solid half-space and a thermoelastic half-space with fractional order derivative. The three-phase lag thermoelastic model [1] is used to discuss the effects of the incident angle and the frequency of the incident wave on the reflection and transmission coefficients in the forms of amplitude ratios and energy ratios, respectively. Finally, comparisons have been made to study the effect of the fractional order parameters, two-phase lag, and three-phase lag theory of thermoelasticity. It is verified that there is no energy dissipation at the interface.

2. Governing Equations

Following Kumar and Gupta [17], the equations of motion, Stress-Strain and temperature relation, and Strain displacement relation are:

$$(\lambda+2\mu)\nabla(\nabla.\mathrm{u})-\mu(\nabla\times\nabla\times\mathrm{u})-\beta_1\nabla T=\rho\ddot{\mathrm{u}}, \tag{1}$$

$$\sigma_{ij}=2\mu e_{ij}+(\lambda e_{kk}-\gamma T)\delta_{ij}, \tag{2}$$

$$e_{ij}=\frac{1}{2}\left(u_{i,j}+u_{j,i}\right). \tag{3}$$

The heat conduction equation for three-phase lag thermoelastic medium with time-fractional derivative is

$$\left[K^*\left(1+\frac{(\tau_v)^\alpha}{\alpha!}\frac{\partial^\alpha}{\partial t^\alpha}\right)+K\frac{\partial}{\partial t}\left(1+\frac{(\tau_T)^\alpha}{\alpha!}\frac{\partial^\alpha}{\partial t^\alpha}\right)\right]\nabla^2 T= \left(1+\frac{(\tau_q)^\alpha}{\alpha!}\frac{\partial^\alpha}{\partial t^\alpha}+\frac{(\tau_q)^{2\alpha}}{(2\alpha)!}\frac{\partial^{2\alpha}}{\partial t^{2\alpha}}\right)\left(\rho C_E\ddot{T}+\gamma T_0\ddot{e}_{kk}\right), \tag{4}$$

where λ,μ are the Lame's constants, ρ is the density assumed to be independent of time, u is displacement vector, α denotes the fractional order parameter, K is the coefficient of thermal conductivity, C_E is the specific heat at constant strain, $T=\Theta-T_0$ is small temperature increment, Θ is the absolute temperature of the medium; T_0 is the reference temperature of the body chosen such that $\left|(T/T_0)\right|<<1$, σ_{ij},e_{ij} are the components of the stress and strain respectively, e_{kk} is the dilatation, $\beta_1=(3\lambda+2\mu)\nu_t,\nu_t$ is the coefficient of thermal linear expansion, τ_q,τ_T and τ_v respectively, are the phase lag of heat flux, phase lag of temperature gradient and phase lag of thermal displacement gradient.

3. Fractional-order derivative and integral

Following Caputo [35] and Miller and Ross [6]:

$$\frac{d^{\alpha}}{dt^{\alpha}} f(t) = I^{1-\alpha} f'(t),$$

where fractional order $\alpha \in (0,1]$ (5)

$$I^{\alpha} f(t) = \int_0^t \frac{(t-\tau)^{\alpha-1}}{\Gamma(\alpha)} f(\tau) d\tau, \quad \alpha > 0. \tag{6}$$

Here $f(t)$ is an absolutely continuous function.

4. Definition and formulation of the problem

We consider a plane interface along the x_1-axis between an isotropic elastic solid half-space $x_3 < 0$ (Medium I) and a thermoelastic solid half-space $x_3 > 0$ (Medium II) with x_3-axis points vertically downwards into the thermoelastic solid medium. The reflection and transmission problem investigated here is in the two-dimensional $x_1 - x_3$ plane. The geometry of the paper is shown in Fig. 1.

Let a plane harmonic wave (P or SV) traveling through the isotropic elastic solid half-space be incident at the interface $x_3 = 0$. The incident wave will give rise to:

(i) Two homogeneous waves (P and SV), reflected in isotropic elastic solid half-space.

(ii) Three inhomogeneous waves (P, T and SV), transmitted in isotropic thermoelastic solid half-space.

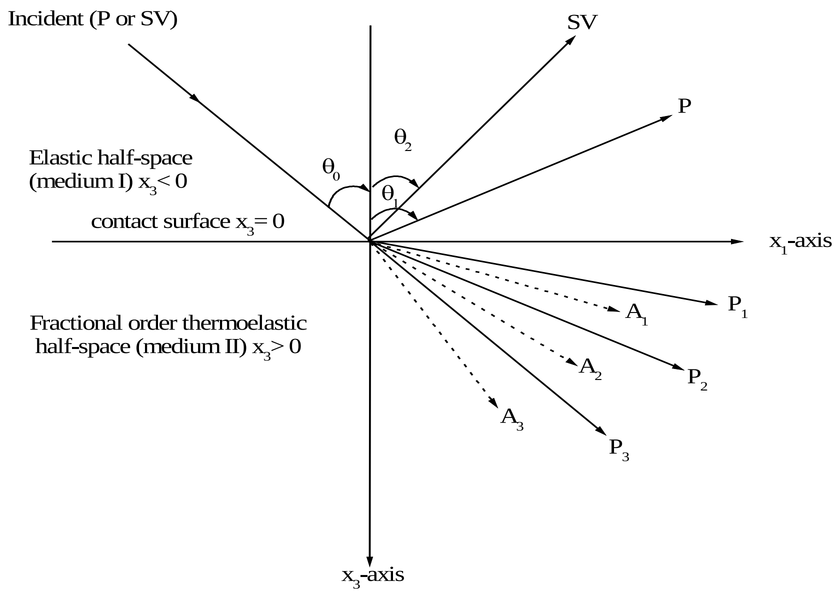

Fig. 1. Geometry of the problem

The displacement vector $\mathbf{u}^e$ of elastic solid half-space and $\mathbf{u}$ of thermoelastic half-space are

$$\mathbf{u}^e = (u_1^e, 0, u_3^e), \mathbf{u} = (u_1, 0, u_3). \tag{7}$$

The dimensionless quantities are introduced as

$$x_i' = C_0\eta x_i, u_i' = C_0\eta u_i, u_i'^e = C_0\eta u_i^e, t' = C_0^{\,2}\eta t, T' = \frac{T}{T_0}, \sigma_{ij}' = \frac{\sigma_{ij}}{\rho C_0^2}, \sigma_{ij}'^e = \frac{\sigma_{ij}^{\ e}}{\rho C_0^2}, P^{*e'} = \frac{P^{*e}}{C_0},$$

$$P_{ij}^{*'} = \frac{P_{ij}^*}{C_0}, \tau_q' = C_0^{\,2}\eta\tau_q, \tau_T' = C_0^{\,2}\eta\tau_T, \tau_\nu' = C_0^{\,2}\eta\tau_\nu, C_T = \frac{1}{C_0}\sqrt{\frac{K^*}{\rho C_E}}, C_K = \sqrt{\frac{\eta K}{\rho C_E}}, \tag{8}$$

$$C_0^{\,2} = \frac{\lambda + 2\mu}{\rho}, i = 1,3.$$

Using Helmholtz representation, the non-dimensional displacement components u_1^e, u_3^e, u_1, u_3 are related by the potential functions as

$$u_1 = (\partial\phi / \partial x_1) - (\partial\psi / \partial x_3), u_3 = (\partial\phi / \partial x_3) + (\partial\psi / \partial x_1),$$

$$u_1^e = (\partial\phi^e / \partial x_1) - (\partial\psi^e / \partial x_3), u_3^e = (\partial\phi^e / \partial x_3) + (\partial\psi^e / \partial x_1). \tag{9}$$

Assuming plane harmonic waves in x_1x_3-plane as

$$\{\phi, \psi, T, \phi^e, \psi^e\}(x_1, x_3, t) = \{\overline{\phi}, \overline{\psi}, \overline{T}, \overline{\phi}^e, \overline{\psi}^e\} e^{-i\omega t}, \tag{10}$$

Where ω is the angular frequency.

Taking $\overline{\phi} = \overline{\phi}_1 + \overline{\phi}_2$, these potentials $\overline{\phi}_1, \overline{\phi}_2$ satisfy the wave equations

$$\left.\begin{aligned} \left[\nabla^2 + \left(\omega^2 / V_1^2\right)\right]\overline{\phi}_1 = 0 \\ \left[\nabla^2 + \left(\omega^2 / V_2^2\right)\right]\overline{\phi}_2 = 0 \end{aligned}\right\} \tag{11}$$

Here V_1, V_2 are the velocities P and T wave in medium 2 and are characteristic roots of the equation

$$FV^4 - E\omega^2 V^2 + D\omega^4 = 0, \tag{12}$$

where

$$F = \beta^2\omega^4 C, E = \beta^2\omega^2 C + \beta^2\omega^2\left(C_T^2 A - i\omega B C_K^2\right) + b \in C\omega^2, D = C_T^2 A - i\omega B C_K^2,$$

$$A = \left(1 + (-i\omega)^\alpha \frac{(\tau_\nu)^\alpha}{\alpha!}\right), B = \left(1 + (-i\omega)^\alpha \frac{(\tau_T)^\alpha}{\alpha!}\right), C = \left(1 + (-i\omega)^\alpha \frac{(\tau_q)^\alpha}{\alpha!} + (-i\omega)^{2\alpha} \frac{(\tau_q)^{2\alpha}}{2\alpha!}\right),$$

$$\in = \frac{\gamma}{\rho C_E}, \beta^2 = \frac{\lambda + 2\mu}{\mu}, b = \frac{\gamma T_0}{\mu}.$$

The potential functions $\overline{\psi}, \overline{\phi}^e, \overline{\psi}^e$ satisfy the equations

$$\left[\nabla^2 + \left(\omega^2 / V_3^2\right)\right]\overline{\psi} = 0, \tag{13}$$

$$\left(\nabla^2 + \omega^2 / v_p^2\right)\overline{\phi}^e = 0, \tag{14}$$

$$\left(\nabla^2 + \omega^2 / v_s^2\right)\overline{\psi}^e = 0, \tag{15}$$

where $V_3 = \dfrac{1}{\beta}$ is the velocity of SV wave in medium 2.

$v_p^e = \sqrt{\dfrac{\left(\lambda^e + 2\mu^e\right)}{\rho^e}}$ and $v_s^e = \sqrt{\dfrac{\mu^e}{\rho^e}}$ are the velocities of P and SV wave in medium 1.

The potential functions in elastic solid half-space(medium 1) are taken as

$$\phi^e = A_0^e \exp\left[i\omega\left\{ \left(\left(x_1 \sin\theta_0 + x_3 \cos\theta_0 \right) / v_p \right) - t \right\} \right] + A_1^e \exp\left[i\omega\left\{ \left(\left(x_1 \sin\theta_1 - x_3 \cos\theta_1 \right) / v_p \right) - t \right\} \right], \tag{16}$$

$$\psi^e = B_0^e \exp\left[i\omega\left\{ \left(\left(x_1 \sin\theta_0 + x_3 \cos\theta_0 \right) / v_s \right) - t \right\} \right] + B_1^e \exp\left[i\omega\left\{ \left(\left(x_1 \sin\theta_2 - x_3 \cos\theta_2 \right) / v_s \right) - t \right\} \right]. \tag{17}$$

where the coefficients $A_0^e\left(B_0^e\right), A_1^e$ and B_1^e are respectively the amplitudes of incident P or incident SV, reflected P, and reflected SV waves.

Following (Borcherdt [15]), in thermoelastic solid half-space (medium 2), the wave field for the transmitted wave is

$$\left\{\phi, T\right\} = \sum_{i=1}^{2} \left\{1, n_i\right\} B_i exp\left(\mathrm{A}_i.\mathrm{r}\right) exp\left\{ i\left(\mathrm{P}_i.\mathrm{r} - \omega t\right)\right\}, \left(i = 1, 2\right) \tag{18}$$

$$\psi = B_3 exp\left(\mathrm{A}_3.\mathrm{r}\right) exp\left\{ i\left(\mathrm{P}_3.\mathrm{r} - \omega t\right)\right\}. \tag{19}$$

Here n_i denotes the constants specified in Appendix 1.

The coefficients B_1, B_2, and B_3 are the transmitted P, T, and SV wave amplitudes.

The propagation and attenuation vectors are

$$\mathrm{P}_i = \xi_R \hat{x}_1 + dV_{iR} \hat{x}_3, \mathrm{A}_i = -\xi_I \hat{x}_1 - dV_{iI} \hat{x}_3,, \left(i = 1, 2, 3\right), \tag{20}$$

$$dV_i = dV_{iR} + i dV_{iI} = p.v.\left(\left(\omega^2 / V_i^2 \right) - \xi^2 \right), \left(i = 1, 2, 3\right), \tag{21}$$

$$\xi = \xi_R + i\xi_I .$$

Here p.v. denotes the principal value.

$$\xi = \left|\mathrm{P}_i\right| \sin\theta_i' - i\left|\mathrm{A}_i\right| \sin\left(\theta_i' - \gamma_i\right), \tag{22}$$

where

$\gamma_i, i = 1, 2, 3$ are the angle between propagation and attenuation vector, $\theta_i', i = 1, 2, 3$ are the angle of refraction.

5. Boundary conditions

At interface x_3 =0,

1. **Mechanical conditions**

Continuity of stress and displacement components

$$\sigma_{33}{}^e = \sigma_{33}, \tag{23}$$

$$\sigma_{31}{}^e = \sigma_{31}, \tag{24}$$

$$u_1{}^e = u_1, \tag{25}$$

$$u_3{}^e = u_3, \tag{26}$$

2. **Thermal condition**

$$\frac{\partial T}{\partial x_3} + hT = 0. \tag{27}$$

where h denotes the coefficient of heat transfer, $h \to 0$ and $h \to \infty$ are respectively for the insulated, and isothermal boundary.

where in equations (23) and (24):

$$\sigma_{31} = \mu\left(u_{1,3} + u_{3,1}\right) / \rho C_0^2, \qquad \sigma_{33} = \left[\left(\lambda + 2\mu\right)u_{3,3} + \lambda u_{1,1} - \rho c_1^2 T - \rho c_1^2 C\right] / \rho C_0^2,$$
$$\sigma_{31}^e = \mu\left(u_{1,3}^e + u_{3,1}^e\right) / \rho C_0^2, \qquad \sigma_{33}^e = \left[\left(\lambda + 2\mu\right)u_{33}^e + \lambda u_{1,1}^e\right] / \rho C_0^2. \tag{28}$$

Using the (16)-(19) in the above equations, we have

$$\sum_{j=1}^{5} d_{ij} Z_j = g_i, \tag{29}$$

and Snell's law

$$\xi_R = \omega \sin\theta_0 / V_0 = \omega \sin\theta_1 / v_p = \omega \sin\theta_2 / v_s, \tag{30}$$

Here Z_1, Z_2 denotes the amplitude ratios of reflected P and reflected SV wave and Z_3, Z_4, Z_5 denotes the amplitude ratios of transmitted P, T and SV waves to that of the incident wave.

Also $d_{ij}, (i, j = 1, 2, 3, 4, 5)$ are specified in Appendix 2.

$$V_0 = v_p^e, \text{when P-wave is incident}$$
$$\text{and} \qquad V_0 = v_s^e, \text{when SV-wave is incident} \tag{31}$$
$$\xi_I = 0$$

The coefficients g_i in the equation (29) are

$$g_i = \begin{cases} (-1)^i d_{i1}, & \textit{for incident P wave} \\ (-1)^{i+1} d_{i2}, & \textit{for incident SV wave} \end{cases} \quad ; i = 1, 2, 3, 4$$
$$g_i = 0; i = 5.$$

6. Energy partition

It is physically important to consider the energy partition of the incident wave among the various reflected and refracted waves at the plane interface. The rate of energy transmission per unit area is given by Achenbach [14]:

$$\left.\begin{aligned} \left\langle P^{*e}\right\rangle &= \operatorname{Re}\left\langle\sigma\right\rangle_{13}^{e} . \operatorname{Re}\left\langle\dot{u}_1^e\right\rangle + \operatorname{Re}\left\langle\sigma\right\rangle_{33}^{e} . \operatorname{Re}\left\langle\dot{u}_3^e\right\rangle \left(\textit{elastic medium}\right) \\ \left\langle P_{ij}^{*}\right\rangle &= \operatorname{Re}\left\langle\sigma\right\rangle_{13}^{(i)} . \operatorname{Re}\left\langle\dot{u}_1^{(j)}\right\rangle + \operatorname{Re}\left\langle\sigma\right\rangle_{33}^{(i)} . \operatorname{Re}\left\langle\dot{u}_3^{(j)}\right\rangle \left(\textit{thermoelastic medium}\right) \end{aligned}\right\} \tag{32}$$

Using equations (16)-(19) in equation (32) with the aid of (9) and (28), we have the energy ratio of reflected P and SV waves as

$$E_i = -\left\langle P_i^{*e}\right\rangle / \left\langle P_0^{*e}\right\rangle; \qquad i, j = 1, 2, \tag{33}$$

and

$$E_{ij} = \left\langle P_{ij}^{*}\right\rangle / \left\langle P_0^{*e}\right\rangle; \qquad i, j = 1, 2, 3, \tag{34}$$

are the energy ratios of transmitted P, T, and SV waves respectively.

The non-diagonal entries

$$E_{RR} = \sum_{i=1}^{3}\left(\sum_{j=1}^{3} E_{ij} - E_{ii}\right). \tag{35}$$

denotes the sharing of interaction energy in all transmitted waves.

Also

$$\left\langle P_1^{*e}\right\rangle = \frac{1}{2}\frac{\omega^4 \rho^e c_0^2}{\alpha}\left|A_1^e\right|^2 \operatorname{Re}\left(\cos\theta_1\right), \left\langle P_2^{*e}\right\rangle = \frac{1}{2}\frac{\omega^4 \rho^e c_0^2}{\beta}\left|B_1^e\right|^2 \operatorname{Re}\left(\cos\theta_2\right),$$

$$\left\langle P_0^{*e}\right\rangle=\begin{cases}\left\langle P_0^{*e}\right\rangle=-\dfrac{1}{2}\dfrac{\omega^4\rho^e c_0^2}{\alpha}\left|A_0^e\right|\cos\theta_0,\left(\text{for incident P}-\text{wave}\right)\\ \left\langle P_0^{*e}\right\rangle=-\dfrac{1}{2}\dfrac{\omega^4\rho^e c_0^2}{\beta}\left|B_0^e\right|\cos\theta_0,\left(\textit{for}\text{ incident SV}-\text{wave}\right)\end{cases},$$

$$\left\langle P_{ij}^{*}\right\rangle=-\frac{\omega^4}{2}\operatorname{Re}\left[\left\{2\mu\frac{dV_i}{\omega}\frac{\xi_R}{\omega}\frac{\bar{\xi}_R}{\omega}+\lambda\left(\frac{\xi_R}{\omega}\right)^2\left(\frac{d\bar{V}_j}{\omega}\right)+\rho c_0^2\left(\frac{dV_i}{\omega}\right)^2\left(\frac{d\bar{V}_j}{\omega}\right)+\frac{\gamma n_i T_0}{\omega^2}\left(\frac{d\bar{V}_j}{\omega}\right)\right\}B_i\bar{B}_j\right],i,j=1,2,3$$

$$\left\langle P_{i3}^{*}\right\rangle=-\frac{\omega^4}{2}\operatorname{Re}\left[\left\{-2\mu\frac{dV_i}{\omega}\frac{d\bar{V}_3}{\omega}\frac{\xi_R}{\omega}+\lambda\left(\frac{\xi_R}{\omega}\right)^2\left(\frac{\bar{\xi}_R}{\omega}\right)+\rho c_0^2\left(\frac{dV_i}{\omega}\right)^2\left(\frac{\bar{\xi}_R}{\omega}\right)+\frac{\gamma n_i T_0}{\omega^2}\left(\frac{\bar{\xi}_R}{\omega}\right)\right\}B_i\bar{B}_3\right],$$

$$\left\langle P_{3j}^{*}\right\rangle=-\frac{\omega^4}{2}\operatorname{Re}\left[\left\{\mu\left(\left(\frac{\xi_R}{\omega}\right)^2\frac{\bar{\xi}_R}{\omega}-\frac{\bar{\xi}_R}{\omega}\left(\frac{dV_3}{\omega}\right)^2\right)-\lambda\frac{\xi_R}{\omega}\frac{dV_3}{\omega}\frac{d\bar{V}_j}{\omega}+\rho c_0^2\frac{\xi_R}{\omega}\frac{dV_3}{\omega}\frac{d\bar{V}_j}{\omega}\right\}\bar{B}_jB_3\right],$$

$$\left\langle P_{33}^{*}\right\rangle=-\frac{\omega^4}{2}\operatorname{Re}\left[\left\{\mu\left(\left(\frac{dV_3}{\omega}\right)^2-\left(\frac{\xi_R}{\omega}\right)^2\right)\frac{d\bar{V}_3}{\omega}-2\mu\frac{\xi_R}{\omega}\frac{\bar{\xi}_R}{\omega}\frac{dV_3}{\omega}\right\}B_3\bar{B}_3\right],\ \text{i , j =1, 2.}\tag{36}$$

The law of conservation of energy is also verified i.e.

$$E_1+E_2+E_{11}+E_{22}+E_{33}+E_{RR}=1.\tag{37}$$

7. Numerical results and discussion

Using the physical data for copper material in a thermoelastic medium (medium 2) are taken from Sherief and Saleh [16] and granite in an elastic medium (medium 1) is taken from Bullen [36].

For thermoelastic medium

$\lambda=7.76\times10^{10}\,Kgm^{-1}s^{-2},\ \mu=3.86\times10^{10}\,Kgm^{-1}s^{-2},\ T_0=0.293\times10^3\,K,$

$C_E=.3831\times10^3\,JKg^{-1}K^{-1},\ \alpha_t=1.78\times10^{-5}\,K^{-1}$

$h=0,\ \rho=8.954\times10^3\,Kgm^{-3},\ K=0.383\times10^3\,Wm^{-1}K^{-1}.$

$C_T=0$ for two and three phase lag model and $C_K=1$.

For elastic medium

$\rho^e=2.65\times10^3\,Kgm^{-3},\ \alpha^e=5.27\times10^3\,ms^{-1},\ \beta^e=3.17\times10^3\,ms^{-1}$

and frequency $\omega=2\times\pi\times100\ Hz$ is kept fixed.

In Figures 2-7 and Figures 8-13, the energy ratios $E_i, i=1,2$ and the energy matrix defined in the previous section are calculated and plotted with respect to the angle of incidence $\theta_0=0°$ to $\theta_0=90°$ for two and three-phase lag models and fractional orders α =0.5 and α =1.5 respectively.

In all figures, the slant and horizontal lines correspond to fractional orders α =0.5 and α =1.5 respectively for three-phase lag model. The horizontal squares and slant squares correspond to fractional orders α =0.5 and α =1.5 respectively for two-phase lag model. The graphs are plotted in 3D to clearly depict the effect of fractional orders and phase lag models.

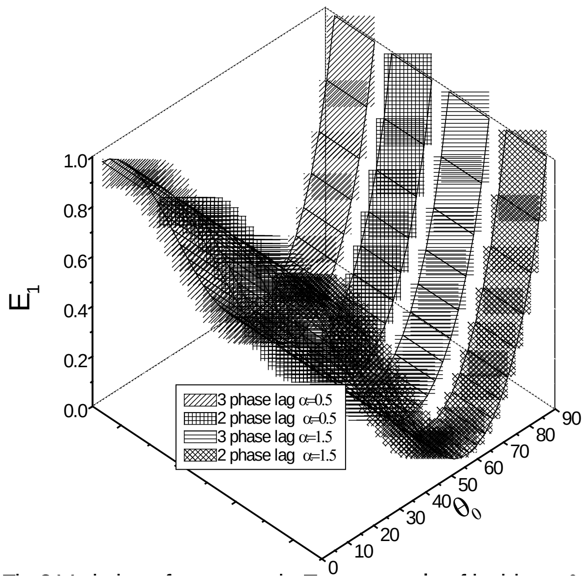

Fig. 2. Variation of energy ratio E_1 w.r.t. angle of incidence θ_0 for P wave

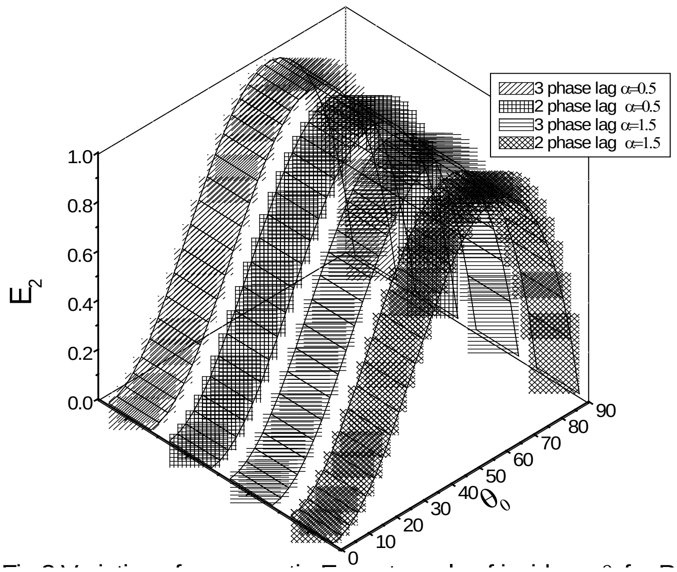

Fig. 3. Variation of energy ratio E_2 w.r.t. angle of incidence θ_0 for P wave

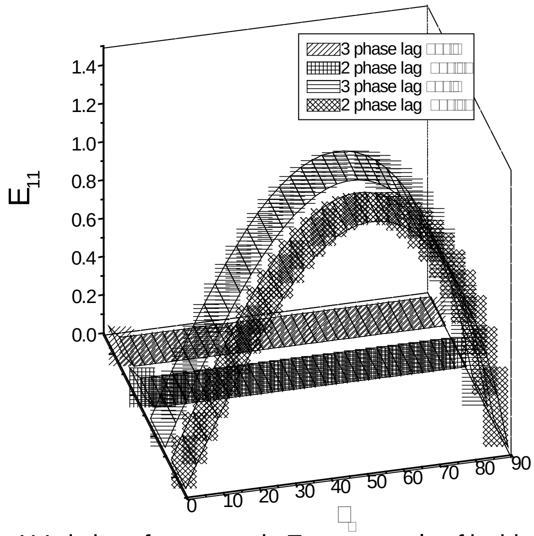

Fig. 4. Variation of energy ratio E_{11} w.r.t. angle of incidence θ_0 for P wave

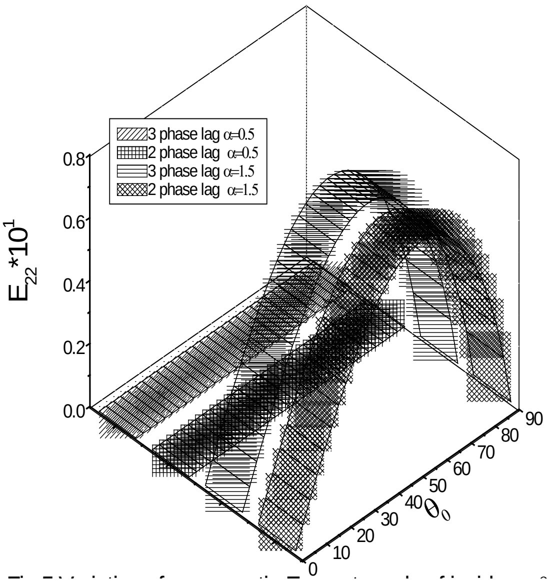

Fig. 5. Variation of energy ratio E_{22} w.r.t. angle of incidence θ_0 for P wave

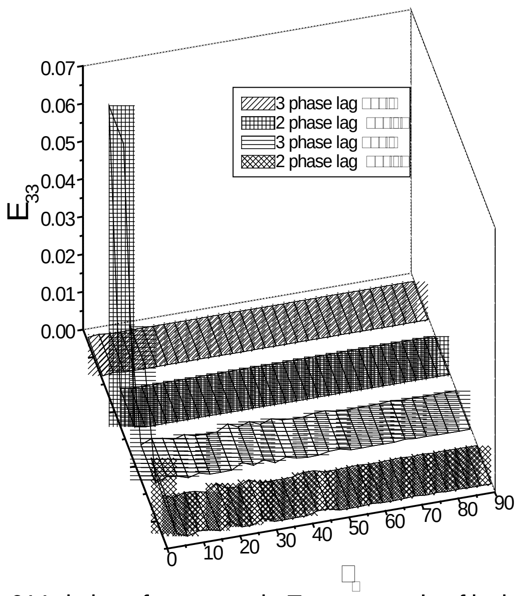

Fig. 6. Variation of energy ratio E_{33} w.r.t. angle of incidence θ_0 for P wave

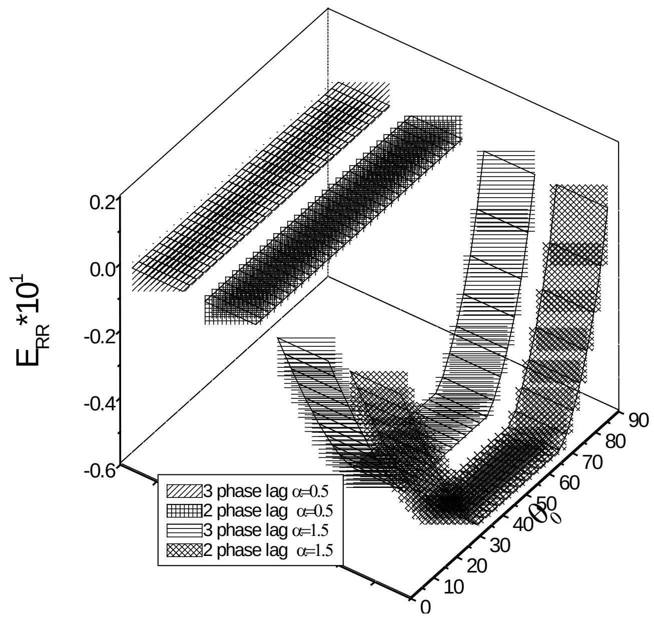

Fig.7. Variation of energy ratio E_{RR} w.r.t. angle of incidence θ_0 for P wave

Incident P wave

Figure 2 depicts that for two and three-phase lag models, for θ_o varies from 0 to 63°, E_1 decreases with increase in θ_o after that E_1 increases with further increase in the values of θ_o up to 90°. But Figure 3 almost depicts the different behavior. Here first E_2 increases in the range $0 \le \theta_o \le 69°$ of θ_o and then decrease in the values of θ_o up to 90°.

Figure 4 indicates that for α =0.5, for both models E_{11} decreases when $0 \le \theta_o \le 5°$ and then attains minima. Due to the small values of E_{11}, its values are magnified after multiplication by 10^6. On the other hand for α =1.5, for both models, E_{11} increases for $0 \le \theta_o \le 69°$ and then decreases continuously. Figure 5 depicts that for α =0.5, for both models E_{22} attains the minimum value. Figure 6 depicts that E_{33} attains the minimum value, nearly to zero in the range $10° \le \theta_o \le 90°$ and in range $0 \le \theta_o \le 10°$ values of E_{33} are higher in the case of two-phase model with α =0.5. The values of E_{33} are magnified by multiplying the original value with 10^{25}. Figure7 depicts that for α =0.5, the energy ratio E_{RR} attains a value nearly equal to zero for both phase models and for α =1.5, E_{RR} decreases in the range $0 \le \theta_o \le 30°$ and attains a constant value in the range $30° \le \theta_o \le 60°$ and further increases rapidly for both phase models. Also from figures, the law of conservation of energy is also verified.

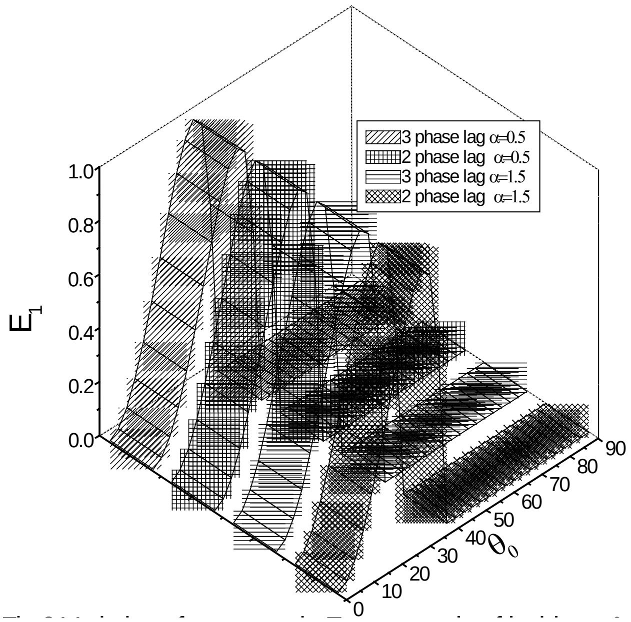

Fig. 8. Variation of energy ratio E_1 w.r.t. angle of incidence θ_0 for SV wave

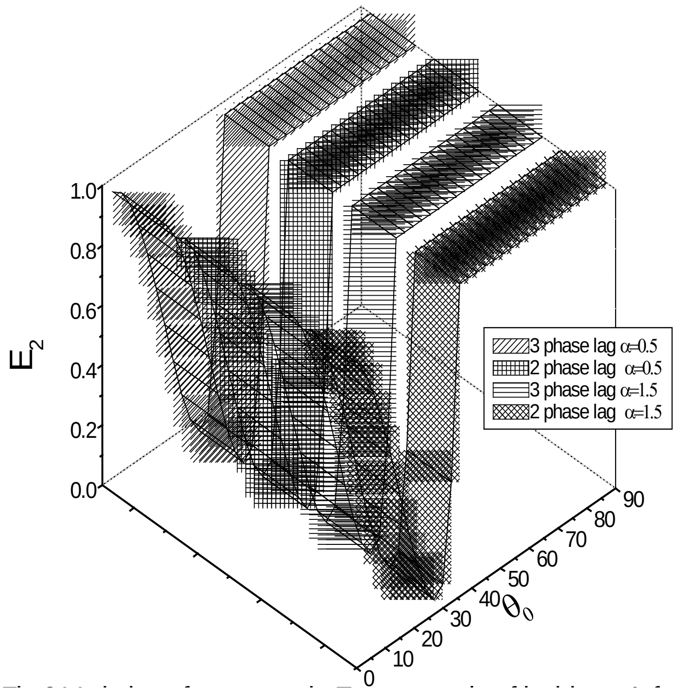

Fig.9. Variation of energy ratio E_2 w.r.t. angle of incidence θ_0 for SV wave

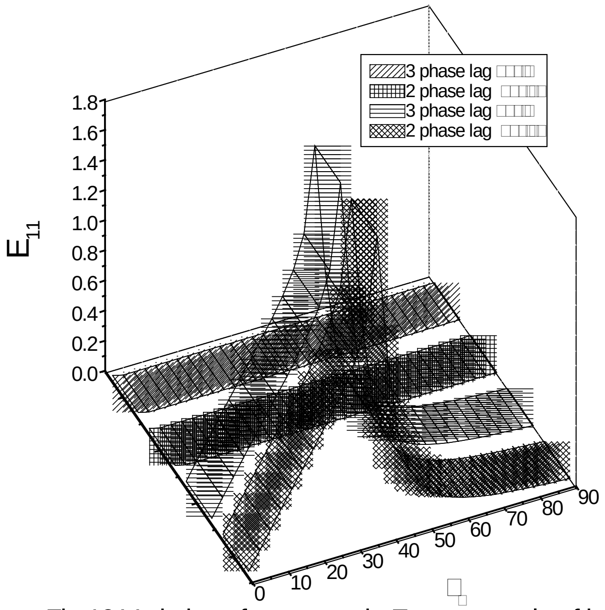

Fig.10. Variation of energy ratio E_{11} w.r.t. angle of incidence θ_0 for SV wave

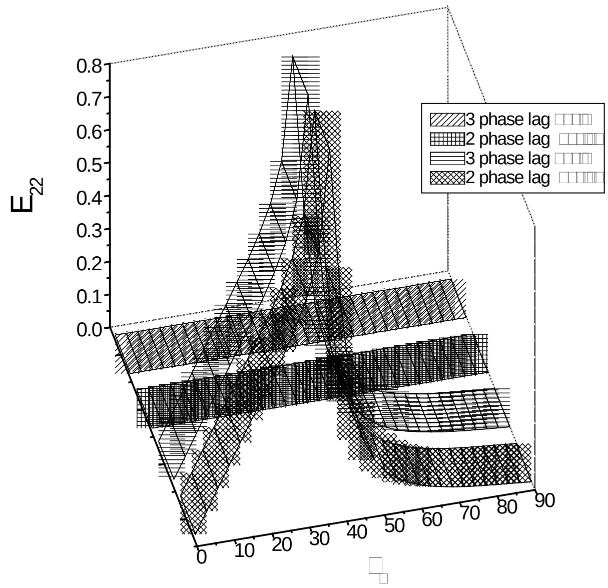

Fig.11. Variation of energy ratio E_{22} w.r.t. angle of incidence θ_0 for SV wave

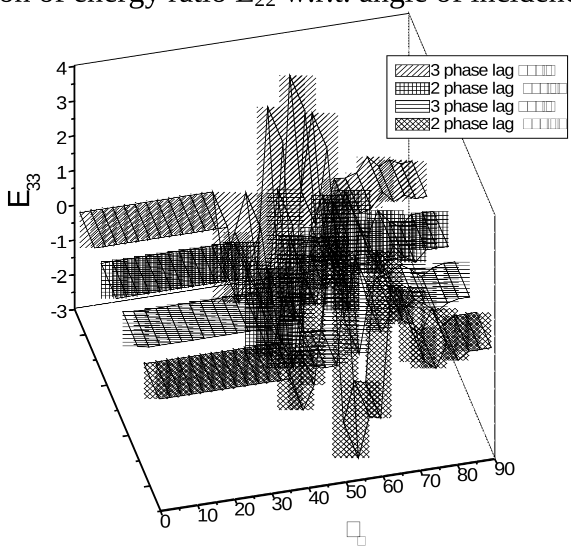

Fig.12. Variation of energy ratio E_{33} w.r.t. angle of incidence θ_0 for SV wave

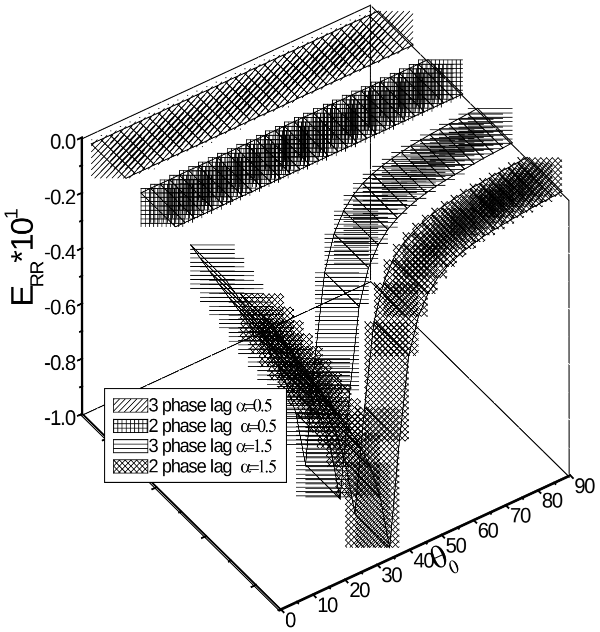

Fig.13. Variation of energy ratio E_{RR} w.r.t. angle of incidence θ_0 for SV wave

Incident SV wave

From Figure 8, it is evident that for both phase models and fractional orders E_1 increases rapidly for $0 \le \theta_o \le 30°$, attains a maximum at $\theta_o = 30°$ and decreases rapidly for $30° \le \theta_o \le 40°$, and thereafter attains minimum value nearly to zero in the range $40° \le \theta_o \le 90°$. From Figure 9 it is clear that the trend of E_2 is opposite to E_1 in the range $40° \le \theta_o \le 90°$. E_{11} and E_{22} shows the same variation for both phase models and fractional orders. Both attain a maximum value of α =1.5 in the range $30° \le \theta_o \le 40°$. The values of E_{11} and E_{22} are magnified by multiplying the original values with 10^6. Figure 12 indicates that E_{33} attains a value nearly to zero in the range $0 \le \theta_o \le 40°$ and then fluctuates for $40° \le \theta_o \le 90°$ and attains maximum and minimum values in the range $40° \le \theta_o \le 60°$. The energy ratios E_{33} are magnified by multiplying the original value with 10^{22}. Figure 13 indicates that for α =0.5 (Two and three-phase lag models) values of E_{RR} are nearly to zero and α =1.5 (Two and three phase lag model), E_{RR} decreases smoothly when $0 \le \theta_o \le 35°$, attains minima at $\theta_o = 35°$ and then increases rapidly in the range $35° \le \theta_o \le 90°$. The law of conservation of energy is verified.

8. Conclusion

1. The reflection/ transmission coefficients of oblique incidence of P (or SV) wave are derived.
2. Reflection/transmission coefficients changes with change in the material parameters and angle of incidence.
3. The results obtained indicate the significant effect of phase lags and fractional parameters on the reflection/transmission characteristics of waves.
4. The energy ratios are numerically calculated and plotted graphically and sum of energy ratios of reflected, and transmitted waves and interference between transmitted waves is proved to be unity which shows that there is no dissipation of energy.

5. Significant effect of fractional orders and phase lag models has been observed on energy ratios.
6. This problem of reflection and transmission of waves has applications in many fields like geophysics, seismology, non-destructive evaluation, etc.

References

1. Roychoudhary SK. On thermoelastic three phase lag model. *Journal of Thermal Stresses*. 2007;30(3): 231-238.
2. Abel NH. Solution de quelques problems a l'aide d'integrales defines. *Werke*. 1823;1: 10
3. Caputo M, Mainardi F. A new dissipation model based on memory mechanism. *Pure and Applied Geophysics*. 1971;91: 134-147.
4. Caputo M, Mainardi F. Linear model of dissipation in anelastic solids. *Rivis ta del Nuovo cimento*. 1971;1: 161-198.
5. Caputo M. Vibrations of an infinite viscoelastic layer with a dissipative memory. *The Journal of the Acoustical Society of America*. 1974;56(3): 897-904.
6. Miller KS, Ross B. *An introduction to the fractional integrals and derivatives, theory and applications*. New York: John Wiley and Sons Inc.; 1993.
7. Lord HW, Shulman Y. A generalized dynamical theory of thermoelasticity. *Journal of the Mechanics and Physics of Solids*. 1967;15(5): 299-309.
8. Green AE, Naghdi PM. A re-examination of the basic postulates of thermomechanics. *Proceedings of Royal Society of America*. *Math. Mathematical, Physical and Engineering Sciences.* 1991;432(1885): 171-194.
9. Green AE, Naghdi PM. On undamped heat waves in an elastic solid. *Journal of Thermal Stresses.* 1992;15(2): 253-264.
10. Green AE, Naghdi PM. Thermoelasticity without energy dissipation. *Jounal of Elasticity*. 1993;31(3): 189-208.
11. Chandrasekharaiah DS. Hyperbolic Thermoelasticity: A review of recent literature. *Applied Mechanics Reviews*. 1998;51: 705-729.
12. Tzou DY. A unified field approach for heat conduction from macro to micro Scales. *Journal of Heat Transfer*. 1995;117: 8-16.
13. Tzou DY. *Macro-to microscale heat transfer: the lagging behavior*. Washigton: Taylor and Francis; 1996.
14. Achenbach JD. *Wave propagation in elastic solids.* North–Holland: Amstendam; 1973.
15. Borcherdt RD. Reflection-refraction of general P and type-I S waves in elastic and anelastic solids. *Geophysical Journal of the Royal Astronomical Society*. 1982;70: 621-638.
16. Sherief HH, Saleh HA. A half space problem in the theory of thermoelastic diffusion. *International Journal of Solids and Structures*. 2005:42: 4484-4493.
17. Kumar R, Gupta V. Wave propagation at the boundary surface of an elastic and thermoelastic diffusion media with fractional order derivative. *Applied Mathematical Modelling*. 2015;39: 1674-1688.
18. Kumar R, Gupta V. Dual-phase-lag model of wave propagation at the interface between elastic and thermoelastic diffusion media. *Journal of Engineering Physics and Thermophysics*. 2015;88: 247-259.
19. Wang YZ, Liu D, Wang Q, Zhou JZ. Fractional Order Theory of Thermoelasticity for Elastic Medium with Variable Material Properties. *Journal of Thermal Stresses*. 2015;38(6): 665-676.
20. Raslan WE. Application of fractional order theory of thermoelasticity to a 1D problem for a spherical shell. *Journal of Theoretical and Applied Mechanics*. 2016;54(1): 295-304.

21. Abbas IA. A dual phase lag model on photothermal interaction in an unbounded semiconductor medium with cylindrical cavity. *International Journal of Computational Materials Science and Engineering*. 2016;5(3): 1650016.
22. Lata P. Fractional order thermoelastic thick circular plate with two temperatures in frequency domain. *Applications and Applied Mathematics*. 2018;13(2): 1216-1229.
23. Kumar R, Vashisth AK, Ghangas S. Waves in anisotropic thermoelastic medium with phase lag, two-temperature and void. *Materials Physics and Mechanics*. 2018;35(1): 126-138.
24. Atwa SY, Ibrahim E. Two temperature effect on a rotational thermoelastic medium with diffusion due to three-phase-lag model. *Journal of Nanotechnology and Advanced Materials,* 2019;7(1): 1-15.
25. Bachher M, Sarkar N. Nonlocal theory of thermoelastic materials with voids and fractional derivative heat transfer. *Waves in Random and Complex Media*. 2019;29(4): 595-613.
26. Mondal S, Sarkar N, Sarkar N. Waves in dual-phase-lag thermoelastic materials with voids based on Eringen's nonlocal elasticity. *Journal of Thermal Stresses*. 2019;42(8): 1035-1050.
27. Said SM. Fractional derivative heat transfer for rotating modified couple stress magneto-thermoelastic medium with two temperatures. *Waves in Random and Complex Media*. 2020;32: 1517-1534.
28. Abouelregal AE. Three-phase-lag thermoelastic heat conduction model with higher-order time-fractional derivatives. *Indian Journal of Physics*. 2020;94: 1949-1963.
29. Abouelregal AE, Ahmad H. A modified thermoelastic fractional heat conduction model with a single-lag and two different fractional-orders. *Journal of Applied and Computational Mechanics*. 2021;7(3): 1676-1686.
30. Saidi A, Abouelregal A. Thermoelastic model with higher-order time-derivatives and two phase-lags for an infinitely long cylinder under initial stress and heat source. *Journal of Applied and Computational Mechanics*. 2021;7(1): 277-291.
31. Kulkarni V, Mittal G. Two temperature dual-phase-lag fractional thermal investigation of heat flow inside a uniform rod. *Applications and Applied Mathematics: An International Journal.* 2021;16(1): 762-775.
32. Abouelregal A, Soleiman A, Sedighi HM, Khalil K, Nasr M. Advanced thermoelastic heat conduction model with two fractional parameters and phase-lags. *Physica Scripta*. 2021;96(12): 124048.
33. Abouelregal A, Alesemi M, Alfadil H. Thermoelastic reactions in a long and thin flexible viscoelastic cylinder due to non-uniform heat flow under the non-fourier model with fractional derivative of two different ordersJ.. *AIMS Mathematics*. 2022;7(5): 8510-8533.
34. Sharma D. Effect of phase-lags model on thermoelastic interactions of nonlocal elastic hollow cylinder with voids material in the presence of time-dependent heat flux. *Proceedings of the National Academy of Sciences, India Section A: Physical Sciences*. 2022;92: 343-352.
35. Caputo M. Caputo Lineal model of dissipation whose q is almost frequency independent II. *Geophysical Journal of the Royal Astronomical Society*. 1967;13: 529-539.
36. Bullen KE. *An introduction to the theory of seismology*. England: Cambridge University Press; 1963.

THE AUTHORS

Puneet Bansal
e-mail: puneet4u@gmail.com
ORCID: 0000-0003-2366-5868

Vandana Gupta
e-mail: vandana223394@gmail.com
ORCID: 0000-0003-2366-5868

Appendix 1

$$n_i = \frac{\beta^2\omega^4 C\overline{\phi}}{\left(\omega^2 C V_i^2 - \omega^2\left(C_T^2 A - i\omega B C_K^2\right)\right)}, \text{ i=1,2.}$$

Appendix 2

$$d_{11} = 2\mu^e\left(\frac{\xi_R}{\omega}\right)^2 - \rho^e c_0{}^2, d_{12} = 2\mu^e\frac{\xi_R}{\omega}\frac{dV_\beta}{\omega}, d_{15} = 2\mu\frac{\xi_R}{\omega}\frac{dV_3}{\omega}, d_{21} = 2\mu^e\frac{\xi_R}{\omega}\frac{dV_\alpha}{\omega},$$

$$d_{22} = \mu^e\left[\left(\frac{dV_\beta}{\omega}\right)^2 - \left(\frac{\xi_R}{\omega}\right)^2\right], d_{25} = \mu\left[\left(\frac{\xi_R}{\omega}\right)^2 - \left(\frac{dV_3}{\omega}\right)^2\right], d_{31} = \frac{\xi_R}{\omega}, d_{32} = \frac{dV_\beta}{\omega},$$

$$d_{35} = \frac{dV_3}{\omega}, d_{41} = -\frac{dV_\alpha}{\omega}, d_{42} = \frac{\xi_R}{\omega}, d_{45} = -\frac{\xi_R}{\omega}, d_{51} = d_{52} = d_{55} = 0,$$

$$d_{1j} = \lambda\left(\frac{\xi_R}{\omega}\right)^2 + \rho c_0{}^2\left(\frac{dV_j}{\omega}\right)^2 + \gamma n_j\frac{T_0}{\omega^2}, d_{2j} = 2\mu\frac{\xi_R}{\omega}\frac{dV_j}{\omega}, d_{3j} = -\frac{\xi_R}{\omega}, d_{4j} = -\frac{dV_j}{\omega},$$

$$d_{5j} = in_j\frac{dV_j}{\omega} + n_j\frac{h}{\omega}, j = 3,4, \frac{dV_\alpha}{\omega} = \left(\frac{1}{\alpha^2} - \left(\frac{\xi_R}{\omega}\right)^2\right)^{\frac{1}{2}} = \left(\frac{1}{\alpha^2} - \frac{\sin^2\theta_0}{V_0{}^2}\right)^{\frac{1}{2}},$$

$$\frac{dV_\beta}{\omega} = \left(\frac{1}{\beta^2} - \frac{\sin^2\theta_0}{V_0{}^2}\right)^{\frac{1}{2}}, \frac{dV_j}{\omega} = p.v.\left(\frac{1}{V_j{}^2} - \frac{\sin^2\theta_0}{V_0{}^2}\right)^{\frac{1}{2}}, \; j = 1, 2, 3.$$